

## Magnetic and magnetocaloric properties of $\text{Ce}_{1-x}\text{R}_x\text{Fe}_2$ and $\text{Ce}(\text{Fe}_{1-x}\text{M}_x)_2$ compounds

This article has been downloaded from IOPscience. Please scroll down to see the full text article.

2010 J. Phys. D: Appl. Phys. 43 285004

(<http://iopscience.iop.org/0022-3727/43/28/285004>)

View [the table of contents for this issue](#), or go to the [journal homepage](#) for more

Download details:

IP Address: 59.162.23.19

The article was downloaded on 05/07/2010 at 06:40

Please note that [terms and conditions apply](#).

# Magnetic and magnetocaloric properties of $\text{Ce}_{1-x}\text{R}_x\text{Fe}_2$ and $\text{Ce}(\text{Fe}_{1-x}\text{M}_x)_2$ compounds

Arabinda Haldar<sup>1</sup>, K G Suresh<sup>1,3</sup> and A K Nigam<sup>2</sup>

<sup>1</sup> Department of Physics, Indian Institute of Technology Bombay, Mumbai-400076, India

<sup>2</sup> Tata Institute of Fundamental Research, Homi Bhabha Road, Mumbai 400005, India

E-mail: [suresh@phy.iitb.ac.in](mailto:suresh@phy.iitb.ac.in)

Received 9 April 2010, in final form 30 May 2010

Published 29 June 2010

Online at [stacks.iop.org/JPhysD/43/285004](http://stacks.iop.org/JPhysD/43/285004)

## Abstract

We have studied selected rare-earth doped and transition-metal doped  $\text{CeFe}_2$  compounds by examining their structural, magnetic and magneto-thermal properties. With substitution of Ce by 5% and 10% Gd and 10% Ho, the Curie temperature can be tuned to the range 267–318 K. Localization of Ce 4f electronic state with rare earth substitutions is attributed for the enhancement of Curie temperature. On the other hand, with Ga and Al substitution at the Fe site, the system undergoes paramagnetic to ferromagnetic transition and then to an antiferromagnetic phase on cooling. The magnetocaloric effect across the transitions has been studied from both magnetization isotherms and heat capacity data. It is shown that by choosing the appropriate dopant and its concentration, the magnetocaloric effect around room temperature can be tuned.

(Some figures in this article are in colour only in the electronic version)

## 1. Introduction

Among the  $\text{RFe}_2$  ( $R$  = Rare earth material) series of compounds  $\text{CeFe}_2$  shows properties which are different compared with the other members of the series [1, 2]. For example, it has anomalous lattice parameter, low Curie temperature ( $T_C = 230$  K) and low saturation magnetization ( $M_s = 2.4\mu_B/\text{f.u.}$ ). Hybridization between 4f and 3d orbitals has been shown to be the main reason behind these anomalies [1].  $\text{CeFe}_2$  is known to be ferromagnetic (FM) with an unstable antiferromagnetic (AFM) ground state. Substitution of selected elements (Ru, Re, Ir, Al, Ga, Si, etc) at the Fe site stabilizes the fluctuating AFM ground state in this material [3–8]. Distinct features of first order transition observed across the AFM to FM transition (on heating) have drawn lots of interest for a long time in these compounds with Fe site substitutions [7–11]. Recently we have shown that Ga-doped compound can also stabilize the AFM ground state in  $\text{CeFe}_2$  compound [7]. Except for a few reports [12], the magnetocaloric properties of Fe-site doped  $\text{CeFe}_2$  compounds

are not probed extensively. Such a study is particularly important in view of the multiple magnetic transitions in them. In this paper, we discuss the magnetocaloric properties of Ga/Al-doped  $\text{CeFe}_2$ , whose magnetic properties were reported very recently.

Regarding the effect of substitutions at the Ce site, only a very few reports are available in the literature which deal with their magnetic properties and so far there are no reports on their magnetocaloric properties. With rare-earth ( $R$ ) substitution, it was shown that one can considerably enhance the  $T_C$  but cannot stabilize the AFM phase at low temperatures [13]. Therefore, rare-earth doped  $\text{CeFe}_2$  compounds still need to be understood for their fundamental aspects. As  $T_C$  can be enhanced with substitution of different rare earths, its magnetocaloric effect (MCE) is also of interest for investigation. Recent interest in the room temperature magnetocaloric effect has given a boost to the research of finding new materials showing large MCE with least hysteresis loss. In view of these, we have studied the magnetic and magnetocaloric properties of  $(\text{Ce}_{1-x}\text{R}_x)\text{Fe}_2$  compounds with  $R = \text{Ho}$  and Gd as well.

The use of a magnetic material as magnetic refrigerant relies on its magnetocaloric behaviour. MCE is a

<sup>3</sup> Author to whom any correspondence should be addressed.

magneto-thermodynamic phenomenon which gives rise to a change in the temperature caused by a material's exposure to a magnetic field. Magnetic entropy change ( $\Delta S_M$ ) and adiabatic temperature change ( $\Delta T_{ad}$ ) are the measure of MCE in a material. It can be measured using magnetization isotherms with the help of Maxwell's relation [14, 15],

$$\Delta S_M(T, \Delta H) = \int_{H_1}^{H_2} \left( \frac{\delta M(T, H)}{\delta T} \right)_H dH. \quad (1)$$

For  $M(H)$  isotherms taken at different constant temperatures at discrete temperature intervals, the above relation can be approximated to the following expression [16]:

$$\Delta S_M \approx \frac{1}{\Delta T} \left[ \int_{H_1}^{H_2} M(T + \Delta T, H) dH - \int_{H_1}^{H_2} M(T, H) dH \right]. \quad (2)$$

Magnetocaloric behaviour can be well parametrized from heat capacity measurement as a function of temperature in constant magnetic fields,  $C(T)_H$ . The entropy of a magnetic solid in zero field and in field can be expressed as [14, 15]

$$S(T)_{H=0} = \int_0^T \frac{C(T)_0}{T} dT + S_0$$

and

$$S(T)_{H \neq 0} = \int_0^T \frac{C(T)_H}{T} dT + S_{0,H}, \quad (3)$$

where  $S_0$  and  $S_{0,H}$  are the zero temperature entropies in zero field and in the presence of a field. In a condensed system these are the same (i.e.  $S_0 = S_{0,H}$ ). Therefore, both  $\Delta T_{ad}(T)_{\Delta H}$  and  $\Delta S_M(T)_{\Delta H}$  can be calculated as [14, 15]

$$\Delta T_{ad}(T)_{\Delta H} \cong [T(S)_{H \neq 0} - T(S)_{H=0}]_S, \quad (4)$$

$$\Delta S_M(T)_{\Delta H} \cong S(T)_{H \neq 0} - S(T)_{H=0}. \quad (5)$$

The quantity that can be used to compare the magnetic refrigeration potential of different materials is the refrigerant capacity or the relative cooling power (RCP) which is parametrized as the product of full width at half maximum of  $\Delta S_M$  versus  $T$  plot and the maximum value of  $\Delta S_M$ .

## 2. Experimental details

All the polycrystalline compounds,  $\text{CeFe}_2$ ,  $\text{Ce}_{0.9}\text{Ho}_{0.1}\text{Fe}_2$ ,  $\text{Ce}_{0.95}\text{Gd}_{0.05}\text{Fe}_2$ ,  $\text{Ce}_{0.9}\text{Gd}_{0.1}\text{Fe}_2$ ,  $\text{Ce}(\text{Fe}_{0.975}\text{Ga}_{0.025})_2$ ,  $\text{Ce}(\text{Fe}_{0.99}\text{Al}_{0.01})_2$  and  $\text{Ce}(\text{Fe}_{0.95}\text{Al}_{0.05})_2$ , were prepared by the arc melting method. The constituent elements, of at least 99.9% purity, were melted by taking their stoichiometric proportion in a water-cooled copper hearth under argon atmosphere. The alloy buttons were remelted several times. The arc melted samples were annealed for 10 days in the following way: 600 °C for 2 days, 700 °C for 5 days, 800 °C for 2 days and 850 °C for 1 day [3]. The structural analysis was performed by the Rietveld refinement of room temperature x-ray diffraction (XRD) patterns. Magnetization and heat capacity measurements were performed in the Physical Property Measurement System (PPMS, Quantum Design Model). Magnetization has been measured in zero-field-cooled (ZFC), field-cooled cooling (FCC) and field-cooled-warming (FCW) modes.

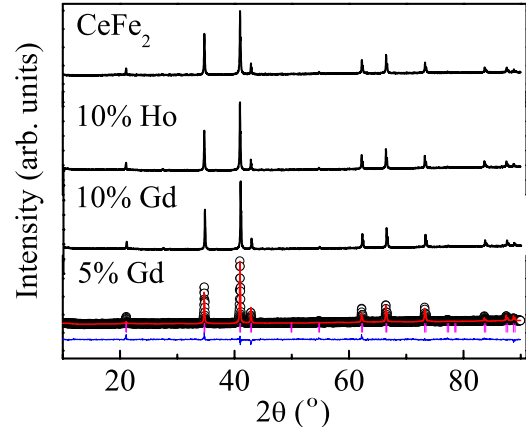


**Figure 1.** Room temperature x-ray diffractograms of  $\text{CeFe}_2$ ,  $\text{Ce}_{0.9}\text{Ho}_{0.1}\text{Fe}_2$ ,  $\text{Ce}_{0.9}\text{Gd}_{0.1}\text{Fe}_2$  and  $\text{Ce}_{0.95}\text{Gd}_{0.05}\text{Fe}_2$  compounds.

## 3. Results and discussion

### 3.1. $(\text{Ce}_{1-x}\text{R}_x)\text{Fe}_2$ [ $R = \text{Gd}, \text{Ho}$ ] compounds

Room temperature XRD patterns are shown in figure 1. Rietveld refinement has been done on all the compounds, but shown only for the 5% Gd-doped compound for clarity in view. Refinement shows that all the compounds, like the parent compound, possess the  $\text{MgCu}_2$  type cubic structure with the space group  $Fd\bar{3}m$  [7].

Temperature variation of magnetization data is shown in figure 2(a) in the 2–330 K range with an applied field  $H = 500$  Oe. The Curie temperature for the undoped  $\text{CeFe}_2$  compound is 228 K which is consistent with an earlier report [17]. All the compounds show FM behaviour in the entire temperature range investigated. This is in contrast to the case of substitutions at the Fe site [3, 4, 7]. With substitution of Ce by 5% and 10% Gd and 10% Ho, the Curie temperature increases from 228 K (for  $\text{CeFe}_2$ ) to 267–318 K. It is observed that for 5% Gd,  $T_C$  is 280 K and for 10% Gd doping, it increases to 318 K. That is, by slightly changing the concentration of rare earths, the  $T_C$  can be varied considerably. In  $\text{CeFe}_2$ , Ce 4f and Fe 3d hybridize and couple ferrimagnetically, which is in contrast to the conventional coupling seen between light rare earth (such as Ce) and the transition elements (such as Fe). This is because, though Ce is a rare earth, its 4f orbital is more or less itinerant. Substitution of rare earth elements at Ce site causes the localization of the 4f electronic state [13]. More localization implies less hybridization between 4f and 3d states which in turn increases the Fe–Fe direct exchange interaction, which is thought to be responsible for the increase in  $T_C$  in the rare earth–transition metal intermetallic compounds.

In figure 2(b) variation of heat capacity data has been shown as a function of temperature, in the 3–295 K range.  $\text{CeFe}_2$  compound shows a sharp peak at  $T_C$  which diminishes with 50 kOe magnetic field.  $C/T$  versus  $T^2$  data at very low temperature show a linear behaviour for  $\text{CeFe}_2$  with an electronic heat capacity coefficient ( $\gamma$ ) value of  $47 \text{ mJ mol}^{-1} \text{ K}^{-2}$  which is consistent with an earlier report [18]. For 5% Gd-doped and 10% Ho-doped  $\text{CeFe}_2$  compound, the  $\gamma$  values are found to be  $44 \text{ mJ mol}^{-1} \text{ K}^{-2}$

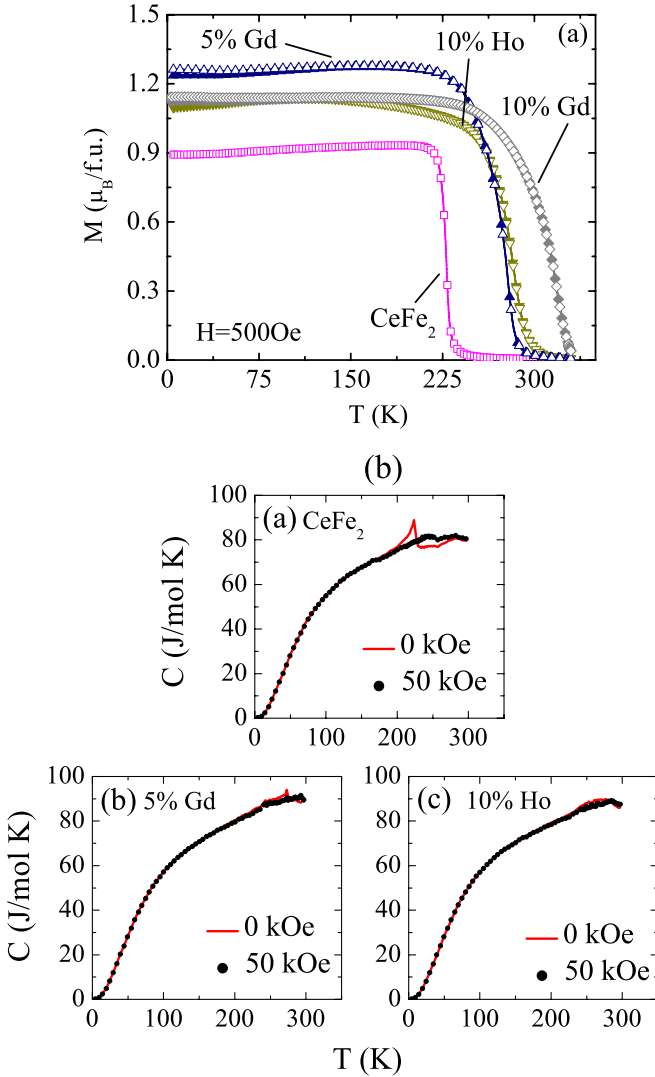


**Figure 2.** (a) Temperature dependence of magnetization of  $CeFe_2$ ,  $Ce_{0.9}Ho_{0.1}Fe_2$ ,  $Ce_{0.95}Gd_{0.05}Fe_2$  and  $Ce_{0.9}Gd_{0.1}Fe_2$  compounds at  $H = 500$  Oe. All the data have been taken during warming the sample both in ZFC (filled symbols) and FCW (open symbols) modes. (b) Heat capacity versus temperature plots for selected compounds in zero and 50 kOe fields. Data have been taken in the ZFC mode.

and  $41 \text{ mJ mol}^{-1} \text{ K}^{-2}$ , respectively. The monotonic decreasing trend in the  $\gamma$  value may be due to the increase in the localization of the 4f band. Both the parent and the substituted compounds show a peak near the Curie temperature, indicating the second order nature of the transition. However, it can be seen that the peak gets diminished in the substituted compounds.

Low temperature ( $T = 3$  K),  $M(H)$  isotherms for the undoped and doped  $CeFe_2$  compounds have been plotted in figure 3. The moment values are found to be saturated at 50 kOe. The saturation magnetic moment is found to be  $2.4\mu_B/f.u.$  for  $CeFe_2$  which matches well with earlier reports [1, 2]. All the compounds show FM behaviour. The saturation moment is found to be  $2.4\mu_B/f.u.$ ,  $2.2\mu_B/f.u.$  and  $1.6\mu_B/f.u.$  for  $CeFe_2$ , 5% Gd- and 10% Ho-doped  $CeFe_2$  compounds, respectively. The decrease in the moment with  $R$  substitution

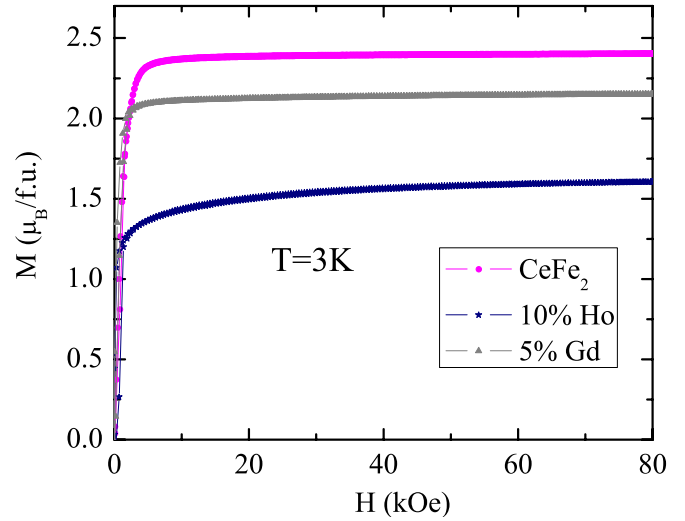


**Figure 3.** Two loop magnetization isotherms at  $T = 3$  K for (Ce, R) $Fe_2$  compounds.

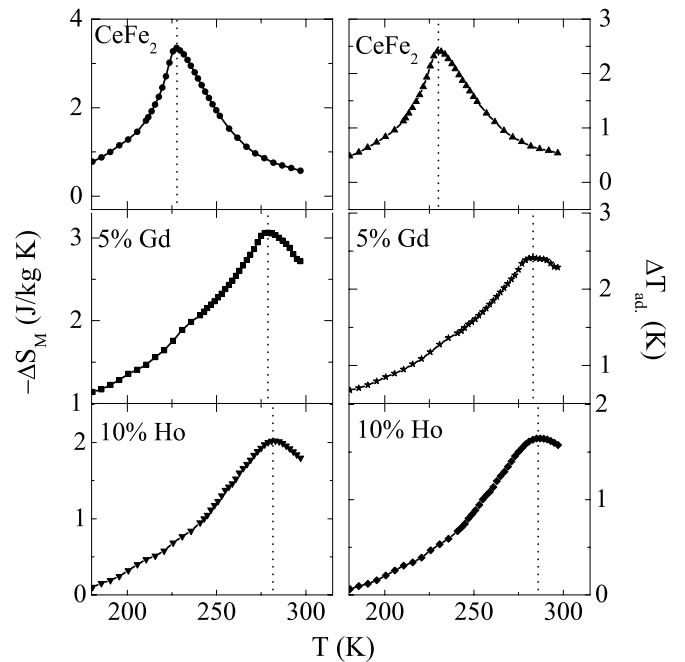


**Figure 4.** (a) Isothermal magnetic entropy change and adiabatic temperature change as a function of temperature in (Ce, R) $Fe_2$  compounds for a field change of 50 kOe.

reflects the fact that the ferrimagnetic coupling between  $R$  and Fe sublattices is more in the doped compounds. The order of transition at  $T_C$  in these compounds can be probed from Arrott's plots [7, 19]. The absence of S-shaped Arrott's plots across the transition temperature region (not shown) indicates the second order phase transition in all these compounds.

MCE has been calculated in terms of isothermal magnetic entropy change ( $-\Delta S_M$ ), using the magnetization isotherms (equation (2)) and using heat capacity data (equation (4)). In the left panel of figure 4 magnetic entropy change, which was calculated from the  $C-H-T$  data, is shown. It is to be noted here that the  $-\Delta S_M$  value is found to be the same as that obtained from the  $M-H-T$  data. Substitution of  $R$  in the place of Ce causes a decrease in  $\Delta S_M$  values. However, the peak

**Table 1.** Curie temperatures ( $T_C$ ), maximum change in entropy ( $-\Delta S_M^{\max}$ ), maximum adiabatic temperature change ( $\Delta T_{\text{ad}}^{\max}$ ) and RCP in  $\text{CeFe}_2$  and rare-earth-doped  $\text{CeFe}_2$  compounds, for a field change of 50 kOe.

Compound	$T_C$ (K)	$-\Delta S_M^{\max}$ ( $\text{J kg}^{-1} \text{K}^{-1}$ ) ( $\Delta H = 50 \text{ kOe}$ )	$\Delta T_{\text{ad}}^{\max}$ (K) ( $\Delta H = 50 \text{ kOe}$ )	RCP ( $\text{J kg}^{-1}$ )
$\text{CeFe}_2$	228	3.8	2.4	141
$\text{Ce}_{0.9}\text{Ho}_{0.10}\text{Fe}_2$	283	1.9	2.4	112
$\text{Ce}_{0.95}\text{Gd}_{0.05}\text{Fe}_2$	280	2.1	1.6	120
$\text{Ce}_{0.9}\text{Gd}_{0.10}\text{Fe}_2$	318	1.6	<sup>a</sup>	108

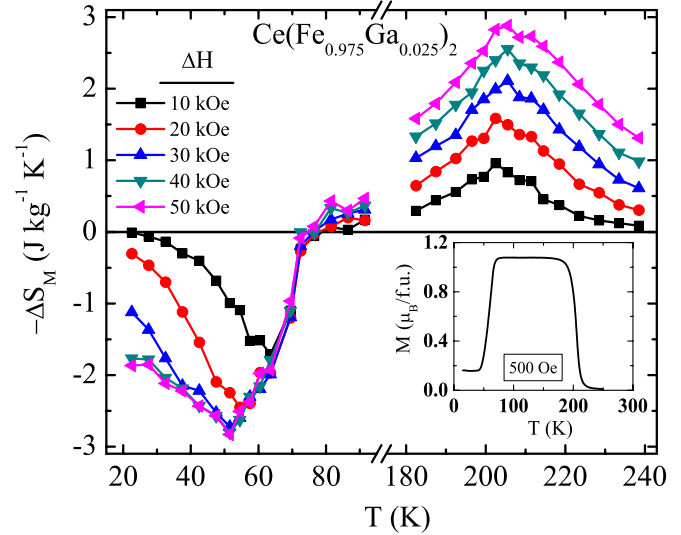
<sup>a</sup> Not measured as the  $T_C$  is close to the safe upper limit of the variable temperature insert of PPMS.

becomes broader, which is necessary for a good refrigerant material. Moreover, different  $R$  substitutions give a MCE peak over a broad temperature region near the room temperature, without much change in the peak value. The values of maximum entropy change ( $-\Delta S_M^{\max}$ ) for  $\Delta H = 50 \text{ kOe}$  have been listed in table 1. Adiabatic temperature change,  $\Delta T_{\text{ad}}$ , has been calculated (equation (5)) from the  $C$ - $H$ - $T$  data and is shown in the right panel of figure 4. For  $\text{CeFe}_2$  the maximum adiabatic temperature change ( $\Delta T_{\text{ad}}^{\max}$ ) is observed to be 2.4 K at 230 K. It is noteworthy here that with 10% Ho substitution, the  $T_C$  has increased to 283 K, but the  $\Delta T_{\text{ad}}^{\max}$  remains unchanged at 2.4 K. For Gd-doped compound this value is slightly less than 2 K. Another parameter of interest for magnetic refrigerant materials is the low hysteresis near the MCE peak region.  $M(H)$  isotherms have been taken during increasing and decreasing fields to calculate the hysteresis loss, which turns out to be almost zero in all the compounds. The quality factor of a refrigerant material is the refrigeration capacity or RCP. RCP for these compounds has been calculated by taking the product of maximum entropy change and full width at half maximum (FWHM) of  $\Delta S_M$  versus  $T$  curves [20] as discussed in the section 1.  $\Delta S_M$  versus  $T$  plot was extrapolated to draw a full envelope around the peak value of  $\Delta S_M$  for calculating FWHM. RCP values thus calculated are tabulated in table 1. The increase in the FWHM is due to the random distribution of the substituted atoms, which produces a distribution of magnetic transition temperatures.

### 3.2. $\text{Ce}(\text{Fe}_{1-x}\text{M}_x)_2$ [ $M = \text{Ga}, \text{Al}$ ] compounds

Although ‘ $R$ ’ substitution at Ce site cannot stabilize the low temperature AFM state, certain substitution at Fe site stabilizes it. This gives rise to FM-paramagnetic (PM) and AFM-FM transitions in such materials. We use Ga/Al-substituted compounds namely,  $\text{Ce}(\text{Fe}_{0.975}\text{Ga}_{0.025})_2$ ,  $\text{Ce}(\text{Fe}_{0.99}\text{Al}_{0.01})_2$  and  $\text{Ce}(\text{Fe}_{0.95}\text{Al}_{0.05})_2$  to study the MCE variation across these transitions. We have recently shown that Ga-substituted  $\text{CeFe}_2$  compound undergoes an AFM transition below  $T_C$  [7]. It was also found that the  $T_C$  decreases with the increase in Ga concentration.

Temperature dependence of magnetization data shown in the inset of figure 5 shows that  $\text{Ce}(\text{Fe}_{0.975}\text{Ga}_{0.025})_2$  undergoes PM to FM transition at  $T_C = 206 \text{ K}$  and FM to AFM phase at the Neel temperature ( $T_N$ ) = 64 K. We have calculated the magnetic entropy change using magnetization isotherms across both these transition regions in this compound, as shown in figure 5. Interestingly the sign of the MCE is different in

**Figure 5.** Isothermal negative magnetic entropy change ( $-\Delta S_M$ ) as a function of temperature in  $\text{Ce}(\text{Fe}_{0.975}\text{Ga}_{0.025})_2$  compound. The inset shows the  $M$ - $T$  data in 500 Oe field.

the two transition regions, resulting in an oscillatory MCE behaviour. This is expected because of the fact that the transitions are AFM-FM and FM-PM in nature. The entropy change is positive across the AFM to FM transition region and it is negative across the FM to PM transition region. The  $-\Delta S_M$  peak across the AFM-FM transition region is found to shift considerably towards a lower temperature with the increase in the field. This is a reflection of the decrease in the Neel temperature with the increase in the field, as usually seen in antiferromagnets. As maximum entropy change occurs at the transition region MCE peak shifts to lower temperatures. The entropy change values are tabulated in table 2. The RCP in this case is found to be more than that of Ru-doped  $\text{CeFe}_2$  compound [12]. Across the PM-FM (FM-AFM) transition RCP value is found to be  $145 \text{ J kg}^{-1}$  ( $127 \text{ J kg}^{-1}$ ) which is  $79.4 \text{ J kg}^{-1}$  ( $59.9 \text{ J kg}^{-1}$ ) in  $\text{Ce}(\text{Fe}_{0.96}\text{Ru}_{0.04})_2$  compound [12]. This difference is expected as the transition is broad in the case of Ga doping compared with Ru doping. It may also be noted that the MCE values are nearly the same in both  $R$ -doped  $\text{CeFe}_2$  as well as in Ga-doped  $\text{CeFe}_2$ .

As mentioned earlier, Al is another substituent which causes the low temperature FM-AFM transition in  $\text{CeFe}_2$ . Therefore, we have calculated the magnetic entropy change in two selected compounds, namely  $\text{Ce}(\text{Fe}_{0.99}\text{Al}_{0.01})_2$  and  $\text{Ce}(\text{Fe}_{0.95}\text{Al}_{0.05})_2$ , whose magnetic properties under pressure

**Table 2.** The maximum change of entropy ( $-\Delta S_M^{\max}$ ) and the RCP in Ga- and Al-doped  $\text{CeFe}_2$  compounds across the FM–AFM and PM–FM transition regions, for a field change of 50 kOe. The quantities in brackets show the uncertainty in the data.

Compound	$T_N$ (K)	$T_C$ (K)	$-\Delta S_M^{\max}$ ( $\text{J kg}^{-1} \text{K}^{-1}$ )		RCP ( $\text{J kg}^{-1}$ )	
			PM–FM	FM–AFM	PM–FM	FM–AFM
$\text{CeFe}_2$	<sup>a</sup>	230	3.8	<sup>a</sup>	141	<sup>a</sup>
$\text{Ce}(\text{Fe}_{0.975}\text{Ga}_{0.025})_2$	64	206	2.8	−2.9	145	127
$\text{Ce}(\text{Fe}_{0.99}\text{Al}_{0.01})_2$	108(5)	178(5)	1.5	−1.8	103	113
$\text{Ce}(\text{Fe}_{0.95}\text{Al}_{0.05})_2$	115(5)	175(5)	1.3	−1.6	98	112

<sup>a</sup> No FM–AFM transition is observed in this case.

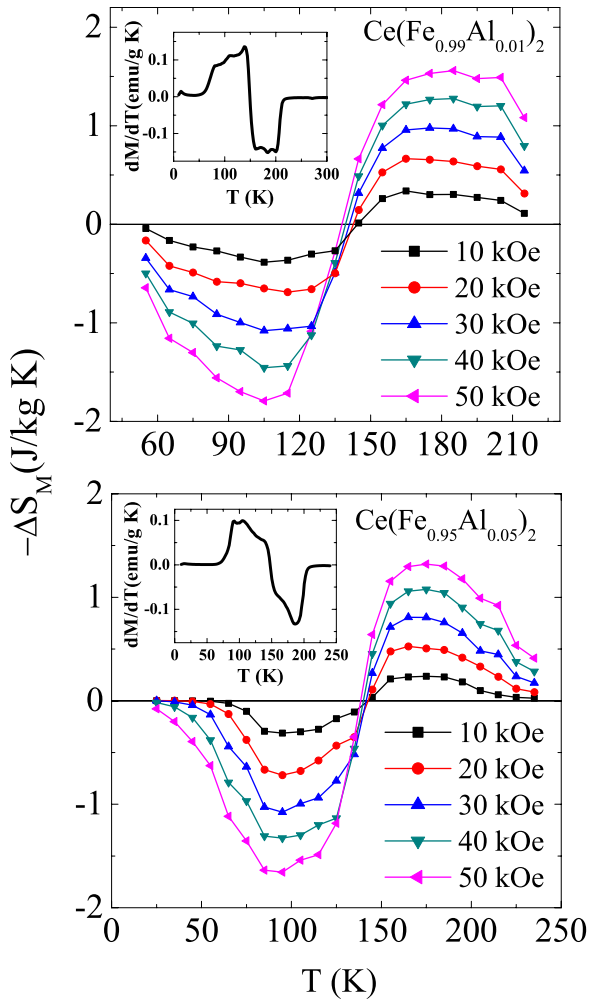


**Figure 6.** ( $-\Delta S_M$ ) versus temperature for  $\text{Ce}(\text{Fe}_{0.99}\text{Al}_{0.01})_2$  and  $\text{Ce}(\text{Fe}_{0.95}\text{Al}_{0.05})_2$  compounds. Insets show  $dM/dT$  versus  $T$  plot for both the compounds.

have been discussed earlier [21]. The AFM–FM and the FM–PM transitions for these two compounds are quite broad in these Al-doped compounds which are shown in the  $dM/dT$  versus  $T$  plots in the insets of figure 6. The oscillatory MCE behaviour is also seen in figure 6. Increase in Al concentration has an effect in reducing the magnetic moment as well as the entropy value. The smaller values of  $-\Delta S_M^{\max}$  compared with Ga-doped compound may come about due to the experimental protocol difference, as in this case, measurement has been taken for a comparatively large temperature step, resulting in the reduction of  $-\Delta S_M^{\max}$ . In the Al-doped compound also

the transitions are broad, which results in comparatively large RCP value although  $-\Delta S_M^{\max}$  is smaller. Table 2 summarizes the MCE values in Ga- and Al-doped compounds, along with the transition temperatures.

As can be seen from the above results, MCE is strongly dependent on the type of magnetic transition. The main difference between Ga- and Al-doped  $\text{CeFe}_2$  compounds is that in the former case, the transition is sharper compared with that of the latter. A clear reflection of this is observed in the MCE, resulting in a rather broad peak in Al-doped compounds compared with the Ga-doped compound. Comparing our results with  $\text{Ce}(\text{Fe}_{0.96}\text{Ru}_{0.04})_2$ , we find that though the MCE value is comparatively small, the RCP value is large in the present case [12]. This may be attributed to the broad magnetic phase transitions in these compounds.

#### 4. Conclusions

We have shown that by substitution of Ce with some selected rare earth elements, one can tune the  $T_C$  towards room temperature. The MCE across the transition region has been studied using the magnetization isotherms and heat capacity data. The  $\Delta S_M^{\max}$  value is found to decrease with rare-earth substitution, but controlled tuning of the MCE peak can be achieved by suitably fixing the rare earth and its concentration. Substitution at the Fe site by Ga and Al causes two transitions, namely PM–FM and FM–AFM. Across these two transition regions,  $\Delta S_M$  shows sign reversal. Broad maxima around the transition temperatures result in larger RCP values. In both the Ce- and the Fe-site-substituted compounds, the magnetocaloric properties seem to be strongly correlated with the magnetic properties. Though the MCE values achieved in this work are not sufficient for commercial applications, the tunability of the MCE and the underlying physics are of importance in the design of novel and potential magnetic refrigerant materials for room temperature applications.

#### Acknowledgments

KGS and AKN thank BRNS for the financial support for carrying out this work. The authors also thank D Buddhikot for his help in certain measurements.

#### References

- [1] Eriksson O, Nordstrom L, Brooks M S S and Johansson B 1988 *Phys. Rev. Lett.* **60** 2523

- [2] Giorgetti C, Pizzini S, Dartyge E, Fontaine A, Baudelet F, Brouder C, Bauer P, Krill G, Miraglia S, Fruchart D and Kappler J P 1993 *Phys. Rev. B* **48** 12732
- [3] Roy S B and Coles B R 1989 *J. Phys.: Condens. Matter* **1** 419
- [4] Roy S B and Coles B R 1989 *Phys. Rev. B* **39** 9360
- [5] Kennedy S J and Coles B R 1990 *J. Phys.: Condens. Matter* **2** 1213
- [6] Rajarajan A K, Roy S B and Chaddah P 1997 *Phys. Rev. B* **56** 7808
- [7] Haldar A, Suresh K G and Nigam A K 2008 *Phys. Rev. B* **78** 144429
- [8] Haldar A, Singh N K, Mudryk Ya, Suresh K G, Nigam A K and Pecharsky V K 2010 *Solid State Commun.* **150** 879–83
- [9] Roy S B, Perkins G K, Chattopadhyay M K, Nigam A K, Sokhey K J S, Chaddah P, Caplin A D and Cohen L F 2004 *Phys. Rev. Lett.* **92** 147203
- [10] Roy S B, Chattopadhyay M K and Chaddah P 2005 *Phys. Rev. B* **71** 174413
- [11] Manekar M A, Chaudhary S, Chattopadhyay M K, Singh K J, Roy S B and Chaddah P 2001 *Phys. Rev. B* **64** 104416
- [12] Chattopadhyay M K, Manekar M A and Roy S B 2006 *J. Phys. D: Appl. Phys.* **39** 1006
- [13] Tang C C, Li Y X, Du J, Wu G H and Zhan W S 1999 *J. Phys.: Condens. Matter* **11** 2027
- [14] Tishin A M and Spichkin Y I 2003 *The Magnetocaloric Effect and Its Applications* (Bristol: Institute of Physics Publishing)
- [15] Pecharsky V K and Gschneidner K A Jr 1999 *J. Magn. Magn. Mater.* **200** 44
- [16] Provenzano V, Shapiro A J and Shull R D 2004 *Nature* **429** 853
- [17] Paolasini L, Dervenagas P, Vulliet P, Sanchez J P, Lander G H, Hiess A, Panchula A and Canfield P 1998 *Phys. Rev. B* **58** 12117
- [18] Pillmayr N, Schaudy G, Holubar T and Hilscher G 1992 *J. Magn. Magn. Mater.* **104–107** 881–2
- [19] Singh N K, Suresh K G, Nigam A K, Malik S K, Coelho A A and Gama S 2007 *J. Magn. Magn. Mater.* **317** 68
- [20] Singh N K, Suresh K G, Nirmala R, Nigam A K and Malik S K 2007 *J. Appl. Phys.* **101** 093904
- [21] Haldar A, Suresh K G, Nigam A K, Coelho A A and Gama S 2009 *J. Phys.: Condens. Matter* **21** 496003